Journal of Pharmaceutical Analysis 12 (2022) 65–76

Contents lists available at ScienceDirect

Journal of Pharmaceutical Analysis

journal homepage: www.elsevier.com/locate/jpa

Original article

Identifying the molecular basis of Jinhong tablets against chronic superficial gastritis via chemical profile identification and symptom-guided network pharmacology analysis

Danfeng Shi [a, 1], Lingxian Liu [a, 1], Haibo Li [b], Dabo Pan [a], Xiaojun Yao [c], Wei Xiao [b, ***], Xinsheng Yao [a, **], Yang Yu [a, *]

[a] Institute of Traditional Chinese Medicine & Natural Products, College of Pharmacy and Guangdong Province Key Laboratory of Pharmacodynamic Constituents of TCM and New Drug Research, Jinan University, Guangzhou, 510632, China
[b] Kanion Pharmaceutical Co., Ltd., State Key Laboratory of New-tech for Chinese Medicine Pharmaceutical Process, Lianyungang, Jiangsu, 222001, China
[c] State Key Laboratory of Quality Research in Chinese Medicine, Macau Institute for Applied Research in Medicine and Health, Macau University of Science and Technology, Taipa, Macau, China

ARTICLE INFO

Article history:
Received 5 June 2020
Received in revised form
27 January 2021
Accepted 27 January 2021
Available online 31 January 2021

Keywords:
Chronic superficial gastritis
Jinhong tablets
UPLC-Q/TOF-MS
Symptom-guided network pharmacology
Molecular docking

ABSTRACT

Chronic superficial gastritis (CSG) is a common disease of the digestive system that possesses a serious pathogenesis. Jinhong tablet (JHT), a traditional Chinese medicine (TCM) prescription, exerts therapeutic effects against CSG. However, the molecular basis of its therapeutic effect has not been clarified. Herein, we employed ultra-performance liquid chromatography coupled with quadrupole time-of-flight tandem mass spectrometry (UPLC-Q/TOF-MS) based chemical profile identification to determine the chemical components in JHT. Further, we applied network pharmacology to illustrate its molecular mechanisms. A total of 96 chemical constituents were identified in JHT, 31 of which were confirmed using reference standards. Based on the bioinformatics analysis using the symptom-guided pharmacological networks of "chi," "blood," "pain," and "inflammation," and target screening through the interaction probabilities between compounds and targets, matrix metalloproteinase 2 (MMP2), dopamine d2 receptor (DRD2), and Aldo-keto reductase family 1 member B1 (AKR1B1) were identified as key targets in the therapeutic effect exhibited by JHT against CSG. Moreover, according to the inhibitory activities presented in the literature and binding mode analysis, the structural types of alkaloids, flavonoids, organic acids, including chlorogenic acid (**10**), caffeic acid (**13**), (−)-corydalmine (**33**), (−)-isocorypalmine (**36**), isochlorogenic acid C (**38**), isochlorogenic acid A (**41**), quercetin-3-*O*-α-L-rhamnoside (**42**), isochlorogenic acid B (**47**), quercetin (**63**), and kaempferol (**70**) tended to show remarkable activities against CSG. Owing to the above findings, we systematically identified the chemical components of JHT and revealed its molecular mechanisms based on the symptoms associated with CSG.

1. Introduction

Chronic superficial gastritis (CSG) is one of the most common diseases of the digestive system [1,2]. As an early stage of stomach disorders, CSG is often characterized by hyperemia, edema, and inflammatory cell infiltration in the gastric mucosa [3]. Besides, it is accompanied by *Helicobacter pylori* infection [4,5]. In the absence of an effective treatment, CSG can lead to fatal diseases, such as peptic ulcer or gastric cancer [6]. Traditional Chinese medicine (TCM) prescriptions against CSG possess several advantages, including early intervention, combination of resistance and protection, and the potential of late recovery owing to comprehensive regulation of microbes and the human body [7].

Jinhong tablet (JHT), a TCM prescription that originated from "Jinlingzi San" in the Yuan Dynasty of Chinese history (1271 AD−1368 AD), is composed of the following four herbs: *Melia*

Peer review under responsibility of Xi'an Jiaotong University.
* Corresponding author.
** Corresponding author.
*** Corresponding author.
E-mail addresses: XWV8501@kanion.com (W. Xiao), tyaoxs@jnu.edu.cn (X. Yao), 1018yuyang@jnu.edu.cn (Y. Yu).
[1] These authors equally contributed to this work.

https://doi.org/10.1016/j.jpha.2021.01.005

toosendan (MT, Chuanlianzi in Chinese), *Corydalis yanhusuo* (CY, Yanhusuo in Chinese), *Vladimiria souliei* (VS, Chuanmuxiang in Chinese), and *Illicium dunnianum* (ID, Honghuabajiao in Chinese). According to the TCM theory, JHT soothes the liver, relieves depression, regulates "chi" (also known as "qi" in Chinese), promotes blood circulation, and relieves pain in the stomach [8]. Clinical studies have also revealed that JHT can reduce the excretion of gastric acid, inhibit the secretion of pepsin, delay gastric emptying, and exhibit significant biological activities, including analgesic, antispasmodic, anti-inflammatory, and anti-gastric ulcer effects [9]. To date, meliacane-type triterpenoids in MT, alkaloids in CY, sesquiterpenoids in VS, and flavonoids in ID have been preliminarily determined to be the main components of the four JHT herbs. Moreover, these components have been found to possess pharmacological activities against CSG [10–13]. However, because JHT is a complex TCM prescription, its therapeutic effect is not a function of a single herb or a single compound; instead, it is the joint action of multiple components and targets. As a result, the chemical profile of JHT is required to clarify its chemical composition and explore the potential active ingredients and mechanism of action that are related to its therapeutic function.

Ultra-performance liquid chromatography coupled with electrospray ionization quadrupole time-of-flight mass spectrometry (UPLC–ESI-Q/TOF-MS) has recently been applied to establish the chemical profile of components by providing high-resolution MS and MS/MS fragmentation information in less run time than conventional method. Owing to characteristics such as accurate mass measurements, high resolution, and excellent sensitivity, UPLC–ESI-Q/TOF-MS has become one of the most effective analytical approaches to rapidly identifying the chemical constituents of TCM prescriptions in vitro or in vivo [14–16].

Network pharmacology has been widely applied to identify the molecular mechanisms employed by multiple components in TCM prescriptions from the perspective of systems biology [17,18]. By encompassing a series of approaches, such as target prediction, bioinformatics analysis, and molecular docking, network pharmacology can effectively reveal the synthetic behaviors of compounds, targets, and signaling pathways. The effects of JHT against CSG are suggested to directly affect "chi" and "blood" in the theory of TCM, and "pain" and "inflammation" in the theory of modern Western medicine [19,20]. Owing to the close relationship between targets and symptoms in TCM prescriptions [21,22], the prediction and screening of targets based on different symptoms would allow us to gain a deeper understanding of the molecular basis of JHT.

In the present study, the chemical profile of JHT was identified via ultra-performance liquid chromatography coupled with quadrupole time-of-flight tandem mass spectrometry (UPLC-Q/TOF-MS) in a rapid and high-throughput manner. Bioinformatics analysis, which was carried out according to symptom-guided network pharmacology, was applied to screen for the key targets of JHT, and the inhibitory activities between key compounds and representative compounds were retrieved from the literature and analyzed via binding mode analysis. The findings herein systematically describe the molecular basis of JHT and reveal its molecular mechanisms based on symptoms associated with CSG.

2. Methods and materials

2.1. Chemicals and reagents

JHT powder (Batch No. 190401; Lianyungang, Jiangsu, China) and its constituent Chinese herbs, MT, CY, VS, and ID, were provided by Kanion Pharmaceutical Co., Ltd. (Lianyungang, Jiangsu, China).

The reference standards, syringin, 4-caffeoyl quinic acid, (−)-stepholidine, (−)-scoulerin, rutin, (−)-corydalmine, (−)-isocorypalmine, cynarin, isochlorogenic acid A, yanhunine, isochlorogenic acid C, (−)-tetrahydroepiberberine, (+)-isocorybulbine, (−)-tetrahydrocoptisine, (−)-tetrahydropalmatine, canadine, (+)-canadaline, 13-methyldehydrocorydalmine, dehydrocorybulbine, and 8-oxoprotoberberine were isolated and identified in our laboratory. Other representative standards, including chlorogenic acid, vitexin-2″-*O*-rhamnoside, isochlorogenic acid B, protopine, (+)-corydaline, palmatine, dehydrocorydaline, costunolide, dehydrocostus lactone, toosendanin, and isotoosendanin, were purchased from Chengdu Must Bio-technology Co., Ltd. (Chengdu, China) (Table S1). A total of 31 reference standards were collected, each with a purity greater than 98%. LC-MS-grade acetonitrile, methanol, and water were purchased from Fisher Scientific (Fair Lawn, NJ, USA). LC-MS-grade formic acid was obtained from Sigma-Aldrich (St. Louis, MO, USA). All other reagents were of analytical grade.

2.2. Preparation of samples and standard solution

First, 30 mg JHT powder and the four Chinese herbs were weighed and dissolved in 1 mL of 50% methanol. After the solution was vortexed for 30 s and centrifuged for 10 min at 14,000 r/min, the supernatant was retrieved for UPLC-Q/TOF-MS analysis. All reference standards were dissolved in methanol to obtain the standard solutions for analysis.

2.3. Instrument and UPLC-Q/TOF-MS conditions

UPLC analyses were carried out with an Acquity UPLC I-Class system equipped with a binary solvent system and an automatic sample manager. Chromatographic separation was achieved with a BEH C_{18} column (2.1 mm × 100 mm, 1.7 μm) at a temperature of 40 °C. The mobile phase consisted of eluent A (water containing 0.1% formic acid, *V*/*V*) and eluent B (acetonitrile containing 0.1% formic acid, *V*/*V*), and the flow rate was set at 0.4 mL/min. The following gradient elution program was adopted: 5%–30% B from 0 to 10 min, 30%–60% B from 10 to 15 min, and 60%–100% B from 15 to 19 min. After holding 100% B from 19 to 21 min, the elution program returned to the starting condition at 5% B. The temperature of the sample room was set to 10 °C, and the injection volume was 2 μL.

The UPLC system was coupled to a hybrid quadrupole-orthogonal time-of-flight (Q-TOF) tandem mass spectrometer (SYNAPT G2 HDMS, Waters, Manchester, U.K.), equipped with electrospray ionization (ESI). The instrument operating parameters were as follows: capillary voltage = 3 kV (ESI+) or −2.5 kV (ESI-), sample cone voltage = 30 V (ESI+) or 40 V (ESI-), extraction cone voltage = 4 V, source temperature = 100 °C, desolvation temperature = 300 °C, cone gas flow = 50 L/h, and desolvation gas flow = 800 L/h. Argon was used as the collision gas for CID in both MS^E and MS^2 modes. To ensure mass accuracy, the full scan mass range was set to 50–1500 Da in both positive and negative modes. Leucine encephalin was used as an external reference, with a constant flow of 5 μL/min using the LockSpray process. As a result, a reference ion at *m/z* 556.2770 in positive ion mode or *m/z* 554.2617 in negative ion mode was generated. During acquisition, the data were centroided.

2.4. Data processing

Data analysis was performed using MassLynx (V4.1, Waters Corporation, Milford, MA, USA). The prediction rules for elemental composition were as follows: maximum tolerance of the mass error = 5 ppm; relative intensity = 5%; degree of unsaturation (DBE) = 5–15, and the atom numbers of carbon, hydrogen, oxygen,

nitrogen, and sulfur = 0–60, 0–100, 0–50, 0–5, and 0–2, respectively [23].

2.5. Analytical strategy for identifying compounds in JHT

Following the retrieval of relevant literature, a chemical database that includes chemical name, molecular formula, exact molecular weight, and structure, was established. Thereafter, 667 known compounds were identified as potential constituents of JHT. The fragmentation pathways and retention time of the reference standards, which were conducive to the identification of compounds in JHT, were subsequently summarized. After each compound in the chemical database was screened using an extracted ion technology according to the self-building chemical database, the source of each observed compound was further characterized via a comparison to the corresponding extracted ion chromatography of the four individual herbs. For a matched chromatographic peak, the most possible chemical structure was identified based on its fragmentation information, the reference standards, and the ChemSpider (http://www.chemspider.com/) and Mass bank (http://www.massbank.jp/) databases, thereby providing a more favorable support for the confirmation. For the unidentified chromatographic peaks, the herb source and formula of these compounds, which were beneficial for characterizing their carbon skeleton, were identified [24]. Thereafter, to verify their structure, the diagnostic ions and characteristic MS/MS patterns were collected for comparison to the corresponding information retrieved from published literature or reference standards [25].

2.6. Target prediction of the chemical constituents in JHT and symptoms of CSG

The 3D structures of 96 chemical constituents in JHT were constructed in Schrödinger Software Suite (Schrödinger, LLC, New York, NY, 2015) and exported in SMILES format. All SMILES were imported into the SwissTargetPrediction webserver (http://www.swisstargetprediction.ch/) for target prediction in "homo sapiens" species [26]. A database was generated for targets that interact with compounds in JHT (database 1), and information regarding the interaction between protein targets and 96 compounds was derived. As the Drugbank database (https://www.drugbank.ca/) provides comprehensive profiles of protein targets associated with approved drugs [27], the protein targets involved in the symptoms associated with CSG were collected using the keywords "mitochondria," "blood," "pain," and "inflammation." Thereafter, a target database for symptoms of CSG (database 2) was constructed. To avoid redundancy in protein targets, the uniport ID of a target was applied as the only identifier for target collection, evaluation, screening, and bioinformatics analysis. The key targets involved in the therapeutic effect of JHT against CSG were selected based on the condition that a key target must interact with the chemical components of JHT and be associated with the symptoms of CSG. A total of 301 targets existing in the overlapping area of database 1 and database 2 were retrieved for further analysis.

2.7. Bioinformatics enrichment analysis and protein-protein interaction analysis of targets involved in the therapeutic effect of JHT against CSG

The key targets involved in the therapeutic effect of JHT against CSG were selected for gene ontology (GO) and Kyoto Encyclopedia of Genes and Genomes (KEGG) analysis via gene set enrichment analysis (GSEA) (version 3.0, http://software.broadinstitute.org/gsea/). Five target datasets (all targets, targets associated with "chi," targets associated with "blood," targets associated with "pain," and targets associated with "inflammation") were analyzed for cellular component, molecular function, biological process, and signaling pathways. Thereafter, items with a false discovery rate below 0.05 were exported. For the target dataset of "all targets," the top 10 items in cellular component, molecular function, biological process, and signaling pathways were analyzed and compared to the items for the target datasets of four symptoms. As for target datasets of four symptoms, the top five items in cellular component, molecular function, and biological process, and top 10 items in signaling pathways were analyzed.

All five target datasets were input into the Search Tool for the Retrieval of Interacting Genes (STRING) database (https://string-db.org/) for protein-protein interaction (PPI) prediction. The species were limited to "*Homo sapiens*" and a "medium confidence score >0.4" was considered to indicate significance. The PPI network was visualized using Cytoscape 3.5 software and analyzed using the Molecular Complex Detection (MCODE) plugin. The parameters for MCODE analysis were as follows: degree cutoff = 2, node score cutoff = 0.2, Kcore = 2, and Max depth = 100. For the "all target" dataset, the significant subnetworks with "MCODE scores ≥5" were extracted from the PPI networks. For target datasets of the four symptoms, the most significant subnetworks with the best MCODE score were extracted from the PPI networks.

2.8. Screening of key targets and construction of the pharmacological network

According to the results of SwissTargetPrediction, the interaction between every compound and every target was evaluated using the term of probability. The importance of each target (termed score) was then determined by calculating the total probability during the interaction with the 96 compounds:

$$Score = \sum_{k=1}^{n} Probability$$

(n=degree, representing the number of interacting compounds).

The key targets in the pharmacological networks of different symptoms were ranked by scores and subsequently screened according to the rank. The symptom-guided pharmacological networks for "chi," "blood," "pain," and "inflammation" were constructed in Cytoscape 3.5 software.

2.9. Molecular docking between representative compounds and targets of JHT

A semi-flexible docking protocol (flexible ligand, rigid protein) was applied to predict the binding modes between the representative compounds and targets in Glide 6.6 of Schrödinger Software Suite (Schrödinger, LLC, New York, NY, 2015). The crystal structures of Aldo-keto reductase family 1 member B1 (AKR1B1; uniport ID: P15121), dopamine d2 receptor (DRD2; uniport ID: P14416), and matrix metalloproteinase 2 (MMP2; uniport ID: P08253) were retrieved from the Protein Data Bank database (https://www.rcsb.org/), with accession numbers 1US0, 6LUQ, and 1HOV, respectively. The initial complex structure was prepared by adding hydrogens, completing missing side chains, and performing minimization in the Protein Preparation Wizard module. Thereafter, the mass centroids of the native ligands (IDD594, risperidone, and SC-74020) were defined as the centers of the binding pockets, which represent the catalytic site of AKR1B1, the substrate binding site of DRD2, and the catalytic site of MMP2, respectively. The 3D structures of compounds **10**, **13**, **33**, **36**, **38**, **41**, **42**, **47**, **63**, and **70**

were constructed and prepared using MMFFs, with a target pH of 7.0 ± 2.0, in the LigPrep module.

The standard precision (SP) protocol was employed to carry out semiflexible docking, with 10 docking runs for all target-compound pairs. The native ligands (IDD594, risperidone, and SC-74020) were first docked to their original binding sites and compared to those of the crystal conformations. The docking scores of native ligands were used as a reference to predict the activity of the representative compounds. The representative compounds were then docked into the binding sites of the three targets and the best docking scores in the docking runs were selected for analysis (Table S2). All other parameters were set as default values.

3. Results and discussion

3.1. Characterization and identification of compounds in JHT using UPLC-Q/TOF-MS

In the present study, a total of 96 compounds were characterized, including 28 alkaloids, 20 organic acids, 16 sesquiterpenoids, 13 triterpenoids, 8 flavonoids, 4 phenylpropanoids, and 7 other compounds. Among them, 31 compounds were unambiguously identified via comparisons to reference standards. The ascriptions of each identified compound were assessed by comparing chromatograms of the Chinese herbs to those of JHT. The base peak intensity (BPI) chromatograms of JHT are depicted in positive and negative ion modes (Fig. 1), and their fragmentation information is presented in Table S3.

3.1.1. Alkaloids

Totally 28 alkaloids from CY, including 14 tetrahydroprotoberberine alkaloids (**22**, **28**, **31**, **33**, **36**, **39**, **43**, **44**, **48**, **49**, **53**, **54**, **58**, **62**), 6 protoberberine alkaloids (**50**, **60**, **61**, **64**, **67**, **68**), 2 protopine alkaloids (**45**, **52**), 2 aporphinoid alkaloids (**34**, **66**), and 4 alkaloids of other types (**25**, **55**, **59**, **77**) were successfully identified in the positive ion mode. Eighteen alkaloids, including 11 tetrahydroprotoberberine alkaloids (**22**, **28**, **33**, **36**, **43**, **48**, **49**, **53**, **54**, **58**, **62**), 4 protoberberine alkaloids (**60**, **61**, **64**, **67**), 1 protopine alkaloid (**45**), and 2 other alkaloids (**59, 77**) were accurately identified using standard compounds.

3.1.2. Flavonoids

Eight flavonoids were detected in JHT, including two flavones (**63**, **70**) and six flavonoid glycosides (**23**, **29**, **30**, **32**, **37**, **42**). Among them, compounds **23**, **29**, **32**, **37**, and **42** are O-glucosyl flavonoids while compound **30** is a C-glucosyl flavonoid.

3.1.3. Organic acids

Organic acids, which possess a carboxyl group as their common structural feature, are another major group of components in JHT. A total of 20 organic acids, including 8 caffeoylquinic acids (**8**, **9**, **11**, **21**, **38**, **40**, **41**, **47**), 3 coumarylquinic acids (**10**, **17**, **20**), 2 phenolic acids (**7**, **14**), and 7 other types of acids (**2, 3**, **4**, **27**, **35**, **46**, **57**) were identified in JHT.

3.1.4. Triterpenoids

The 13 identified triterpenoids (**69**, **73**, **80**, **81**, **84**, **85**, **86**, **88**, **90**, **91**, **94**, **95**, **96**) of JHT were of the limonoid-type and were uniquely derived from MT.

3.1.5. Sesquiterpenoids

Sixteen sesquiterpenoids were detected in JHT. Among them, compounds **71**, **72**, **74**, **75**, **78**, **79**, **82**, **83**, **87**, **89**, **92**, and **93** originated from VS while compounds **8**, **14**, **26**, and **65** originated from ID.

Figs. S1–S4 and Supplementary data further describe the compounds identified in JHT based on UPLC-Q/TOF-MS. The structures of these compounds are presented in Fig. S5. Compound **62** (Fig. 2) was used as an example to describe the identification process. This compound was found to elute at 8.58 min, with an $[M+H]^+$ ion at *m/z* 370.2030 ($C_{22}H_{28}NO_4$). The fragment ions at *m/z* 192.1030 ($C_{11}H_{14}NO_2$) and 179.1068 ($C_{11}H_{15}O_2$) were identified as the products of RDA cleavage while the ion at *m/z* 165.0924 was generated via cleavage of the B-ring. As the daughter ions at *m/z* 354.1710 and 326.1754 could be assigned to the continuous loss of CH_4 (16.0313 Da) and CO (27.9949 Da), two adjacent methoxy substitutions could occur [28]. A series of ions at m/z 176.0719 ($[M + H–C_{11}H_{14}O_2–CH_4]^+$), 149.0605 ($[M + H–C_{12}H_{15}NO_2–CH_4]^+$), 148.0771($[M + H–C_{11}H_{14}O_2–CH_4–CO]^+$), 135.0811 ($[M + H–C_{11}H_{13}NO_2–CH_4–CO]^+$), and 121.0664 ($[M + H–C_{12}H_{15}NO_2–CH_4–CO]^+$) were obtained in the high-energy MS^E spectrum. Because compound **62** had the same retention time and

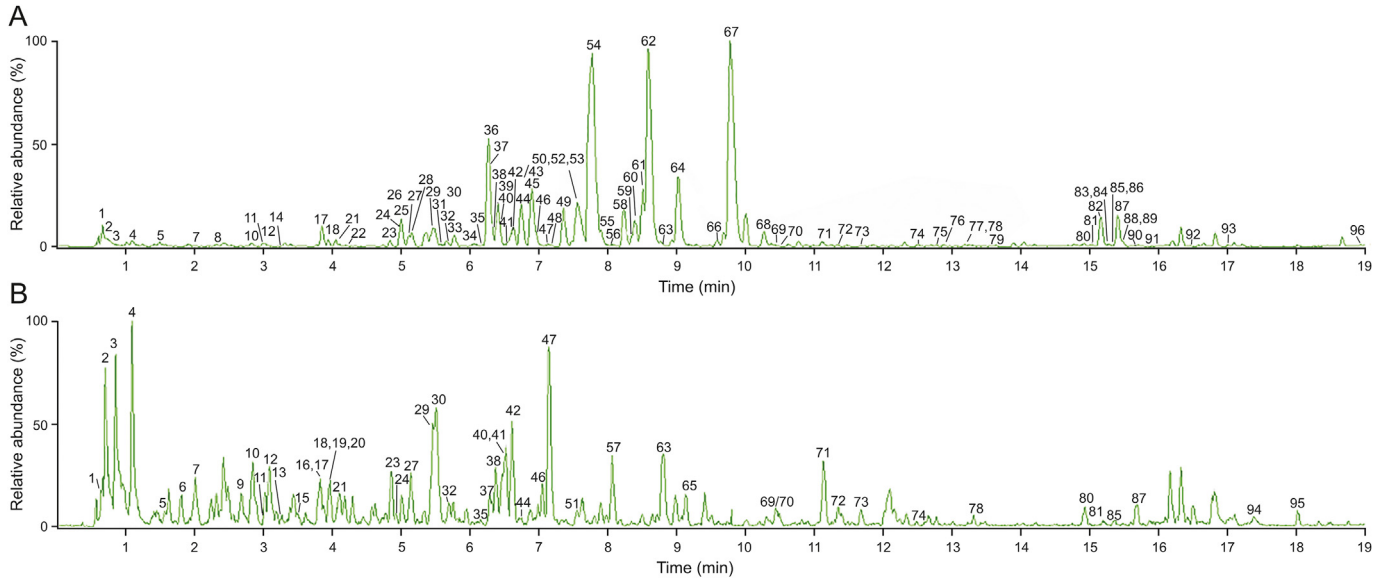

Fig. 1. The base peak intensity (BPI) chromatograms of Jinhong tablet (JHT). (A) (+) ESI-MS chromatogram of JHT and (B) (−) ESI-MS chromatogram of JHT.

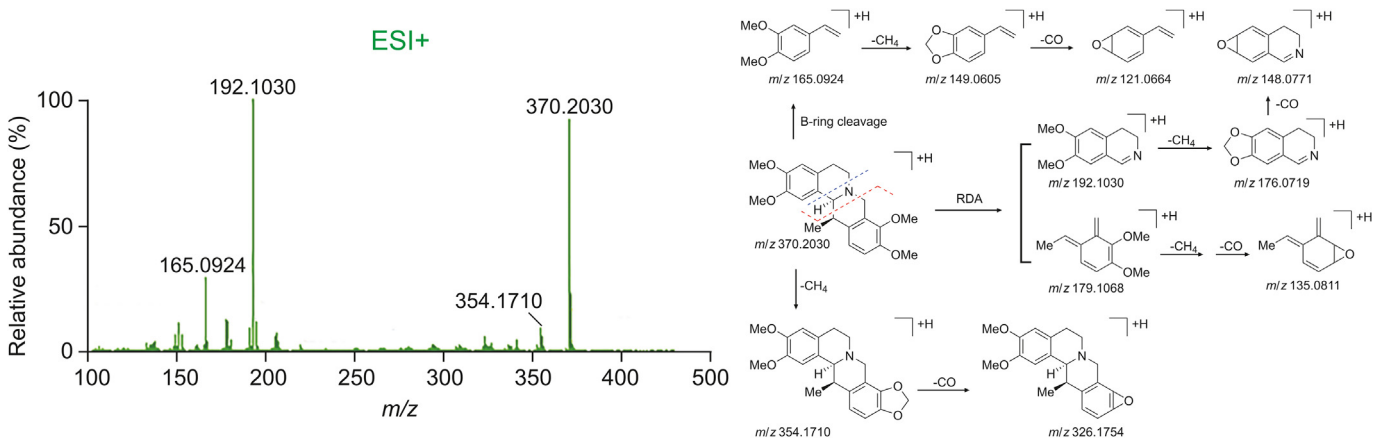

Fig. 2. Detailed fragmentations and proposed fragment pathway for compound **62**.

fragment ions as authentic (+)-corydaline standard, it was unambiguously characterized as (+)-corydaline. Other compounds belonging to the tetrahydroprotoberberine family could be identified by comparing their fragmentation pathways to those of compound **62**.

3.2. Construction of a symptom-guided target database and bioinformatics analysis of the targets involved in the effects exhibited by JHT

When JHT is clinically administered to treat CSG, the target organ (stomach) could directly interact with the chemical components of JHT during administration. As a result, we sought to use all the compounds identified to construct a pharmacological network for JHT and analyze its therapeutic effect against CSG from the perspective of four symptoms, including "chi," "blood," "pain," and "inflammation," "Chi," also known as "vital force or energy," was found to be mainly associated with mitochondrial biology for energy production and is thus referred to as "mitochondria" in the target collection process [29,30]. As shown in Fig. 3A, the target collection workflow was integrated via target prediction using the SwissTargetPrediction server and a target search based on symptoms in the Drugbank database. The target prediction based on SwissTargetPrediction derived 1136 protein targets that form multiple compound-target interactions with 96 compounds (Table S4). In contrast, the target search based on Drugbank derived 249 targets for "chi," 96 targets for "blood," 408 targets for "pain," and 140 targets for "inflammation." The targets collected from the two databases were compared and the common targets were extracted for different symptoms, as shown in Fig. 3B and Table S5. Altogether, 35 targets for "chi," 40 targets for "blood," 192 targets for "pain," and 74 targets for "inflammation" were found to simultaneously interact with the chemical constituents of JHT. Accordingly, these targets might serve as the molecular basis for the therapeutic effect exhibited by JHT against CSG.

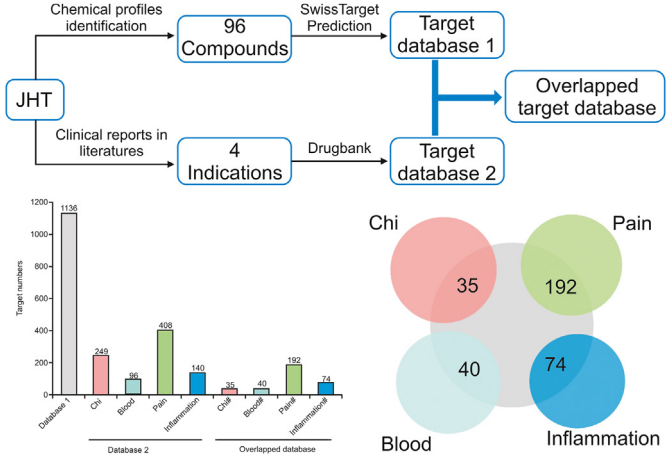

Fig. 3. The symptom-guided target database for the therapeutic effect of JHT against chronic superficial gastritis (CSG). (A) Target collection workflow integrated by target prediction in the SwissTargetPrediction server and target search by symptoms in the Drugbank database. (B) The number of targets in database 1, database 2, and the overlapped database. The target databases for "Chi#," "Blood#," "Pain#," and "Inflammation#" are depicted as the overlapped areas between database 1 and database 2 for the different symptoms.

To determine the biological basis for the therapeutic effect of JHT against CSG, target datasets for non-redundant targets and the four symptoms associated with CSG were input into GSEA for gene enrichment analysis. Thereafter, the relationship between the biological items and symptoms was assessed (Table S6). As shown in Fig. 4, the top 10 items for molecular function, cellular component, biological process, and signaling pathways were extracted according to the rank of the *P* values. However, biological process was found to be mainly involved in the response to compounds, such as oxygen-containing compounds, organic cyclic compounds, nitrogen compounds, and endogenous stimuli (Fig. 4A). As the most important item for the biological process was "response to oxygen containing compound," the metabolism or regulation of these compounds might affect "chi" and "pain." The cellular component and molecular function items showed that the targets were mainly distributed in membrane regions and nerve tissues, including the synapse, neuron, and dendritic tree, which regulate the activity of molecular transducers, receptors, kinases, gated channels, and so on. (Figs. 4B and C). The most important items for molecular function and cellular component were "intrinsic component of plasma membrane" and "molecular transducer activity," respectively. According to KEGG analysis, the most important signaling pathway was "neuroactive ligand receptor interaction"; this finding is consistent with the items of cellular component and molecular functions (Fig. 4D). For different symptoms, the most significant pathways for "chi," "blood," "pain," and "inflammation" were "pathways in cancer," "complement and coagulation cascades," "neuroactive ligand-receptor interaction," and "protein serine threonine kinase activity," respectively (Fig. S6); these pathways displayed good correlations with the different symptoms. Based on gene enrichment analysis, a signaling pathway may be associated

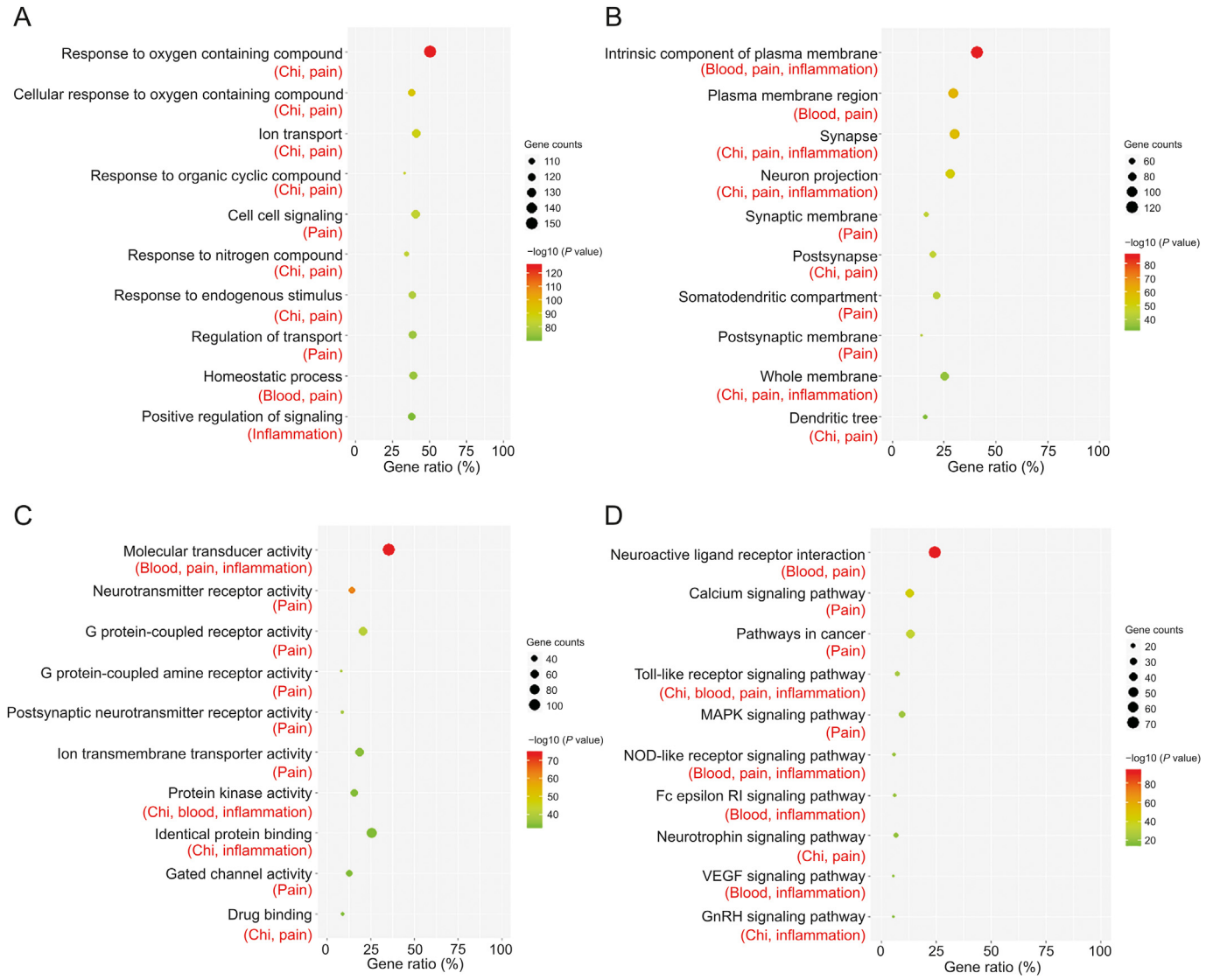

Fig. 4. Gene enrichment analysis of all non-redundant targets (301 targets) involved in the therapeutic effect of JHT against CSG. (A) The top 10 items in the gene ontology (GO) biological process. (B) The top 10 items in the GO cellular component. (C) The top 10 items in the GO molecular function. (D) The top 10 items in Kyoto Encyclopedia of Genes and Genomes (KEGG) signaling pathway. The four symptoms (chi, blood, pain, and inflammation) associated with the extracted items are displayed below the item names.

with multiple symptoms, and the comprehensive interactions of these biological items ensure that JHT exhibits a therapeutic effect against CSG.

By analyzing the protein-protein interactions between the non-redundant targets (301 targets), five key subnetworks (MCODE scores $\geq$ 5) were extracted, as shown in Fig. 5. Each subnetwork was identified to contain targets from the dataset associated with "chi," "blood," "pain," and "inflammation." The targets involved in more than one symptom were subnetwork 1: PTGDR2, GPR55, GPER1, APP, CNR2; subnetwork 2: BCL2L1, NR3C1, NOS2, CASP1, LTB4R, F2, PPARG, VCAM1, MMP2, IL1B; subnetwork 3: PLG, ALOX5, IKBKB, PTGS2, ALB, VEGFA, IL6, PGR, MAPK14, SYK; subnetwork 4: GSR; subnetwork 5: ALOX15, BCL2. Compared to the most significant subnetwork in each symptom dataset, GPER1 was found to be involved in the subnetwork for "chi" (Fig. S7); F2, MMP2, ALB, VEGFR, IL6, and MAPK14 were involved in the subnetwork for "blood" (Fig. S8); PTGDR2, GPR55, and CNR2 were involved in the subnetwork for "pain" (Fig. S9); and NOS2, CASP1, IL1B, PLG, SYK, PPARG, VCAM1, ALOX5, IKBKB, and PTGS2 were involved in the subnetwork for "inflammation" (Fig. S10). Accordingly, these targets were the key hubs in the protein-protein interactions of the four symptoms.

3.3. Target screening in the symptom-guided pharmacological network for JHT

The pharmacological networks for "chi," "blood," "pain," and "inflammation" (Figs. S11–S14) revealed that the key targets for each symptom interacted with multiple chemical components from the four herbs found in JHT, including the structural types of alkaloids, flavonoids, organic acids, and sesquiterpenoids. As shown in Table S7, the possible interactions between compounds and targets were set as a weight factor to evaluate the importance of a target for each symptom. Targets with better scores were extracted to explain the comprehensive regulatory effect of JHT. As shown in Table 1, the top three targets in each symptom-guided pharmacological network were: SIGMAR1, MMP2, and APP in the chi-associated pharmacological network; F3, MMP2, and SYK in the blood-associated pharmacological network; MMP2, APP, and ALOX5 in the inflammation-associated pharmacological network;

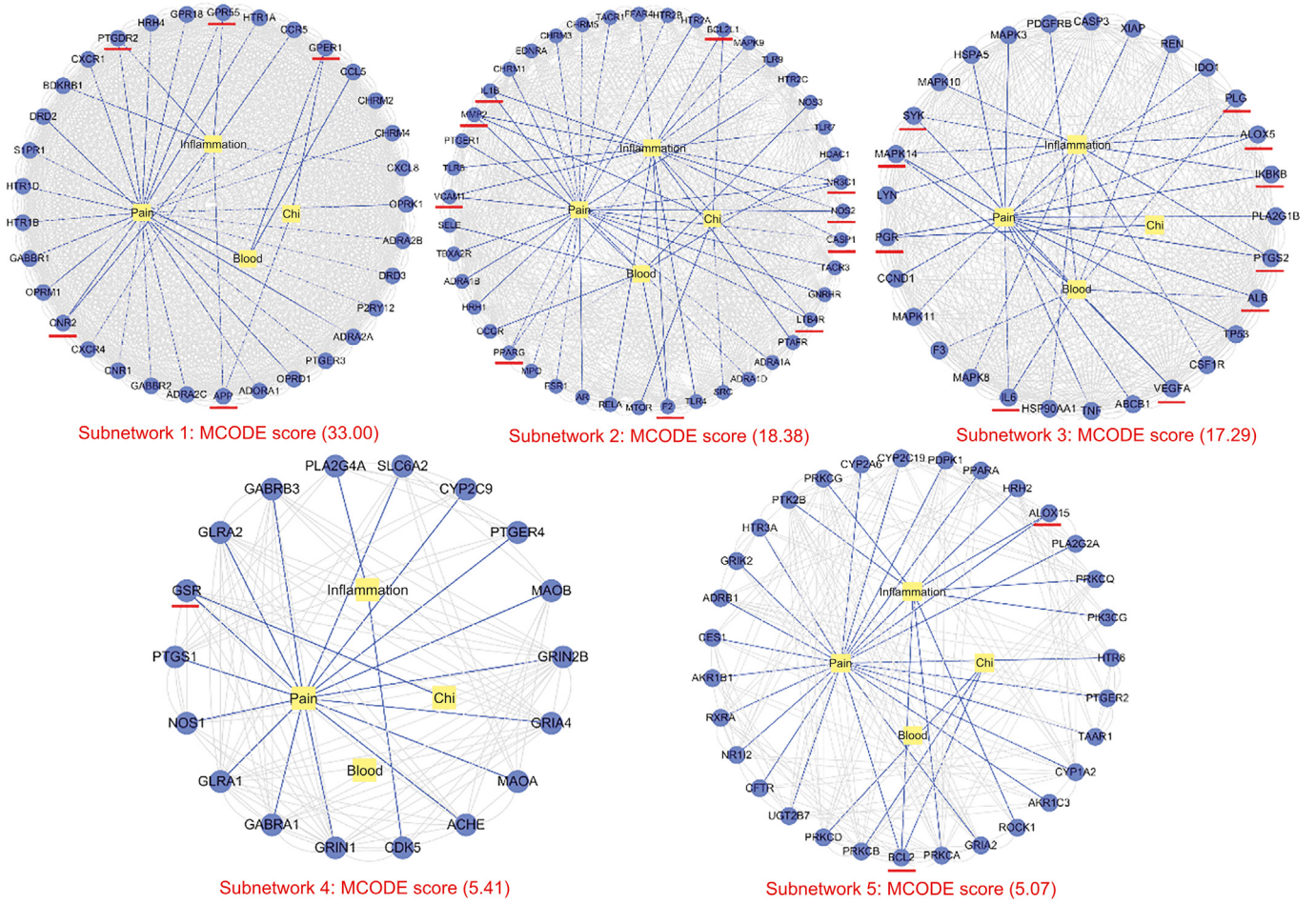

Fig. 5. Key subnetwork analysis of the protein-protein interaction (PPI) for all non-redundant targets (301 targets) involved in the therapeutic effect of JHT against CSG. Five subnetworks (MCODE scores ≥ 5) were extracted and the targets associated with more than one symptom are displayed as red lines.

Table 1
Detailed information for the screened targets involved in chronic superficial gastritis (CSG)-associated symptoms, such as "chi," "blood," "pain," and "inflammation" based on scoring evaluation and an analysis of their association with gastritis.

Gene name	Protein class	Symptoms	Degree[a]	Score[b]	Selection standard[c]
SIGMAR1	Membrane receptor	Chi	41	12.02	Top 3 target for symptom
MMP2	Protease	Chi, blood, inflammation	34	6.70	Top 3 target for symptom
APP	Membrane receptor	Chi, inflammation	26	5.67	Top 3 target for symptom
F3	Protease	Blood	38	13.04	Top 3 target for symptom
SYK	Kinase	Blood	34	2.84	Top 3 target for symptom
ALOX5	Oxidoreductase	Inflammation	37	5.56	Top 3 target for symptom
DRD1	Family A GPCR	Pain	25	13.68	Top 3 target for symptom
DRD2	Family A GPCR	Pain	35	13.47	Top 3 target for symptom, drug target for gastritis
AKR1B1	Enzyme	Pain	41	14.41	Top 3 target for symptom, drug target for gastritis
CHRM1	Family A GPCR	Pain	24	1.87	Drug target for gastritis
CHRM4	Family A GPCR	Pain	32	4.16	Drug target for gastritis
TYMS	Transferase	Chi	36	1.54	Drug target for gastritis
DRD3	Family A GPCR	Pain	33	11.20	Drug target for gastritis
TUBB1	Structural protein	Pain	20	1.42	Drug target for gastritis
HTR1A	Family A GPCR	Pain	33	10.20	Drug target for gastritis
HTR2A	Family A GPCR	Pain	38	4.44	Drug target for gastritis
PTGS1	Oxidoreductase	Pain	37	1.73	Drug target for gastritis
PTGS2	Oxidoreductase	Pain, inflammation	54	4.07	Drug target for gastritis
MPO	Enzyme	Pain	19	1.96	Drug target for gastritis
XDH	Oxidoreductase	Pain	8	2.64	Drug target for gastritis
SLC18A2	Electrochemical transporter	Pain	18	1.60	Drug target for gastritis

[a] Number of compounds in JHT that interact with a target.
[b] Score derived according to the sum of the probabilities of a target that interact with different compounds.
[c] The selection standards are based on two aspects: 1) target ranking of the top 3 based on scoring evaluation for the symptom; and 2) the target associated with gastritis according to the Drugbank and OMIM databases.

and DRD1, DRD2, and AKR1B1 in the pain-associated pharmacological network. Among these targets, MMP2 tended to be an important target in "chi," "blood," and "inflammation." MMP2 is a type of matrix metalloproteinase with several functions, including vasculature remodeling, angiogenesis, tissue repair, tumor invasion, inflammation, and atherosclerotic plaque rupture [31]. Previously, the expression level of MMP2 was found to significantly differ between the gastritis tissue and normal tissue [32–34], thereby proving its potential as a biomarker. To date, many drugs used to treat gastritis have been approved by the United States Food and Drug Administration (FDA). Moreover, the associated targets reported in the OMIM and Drugbank databases were collected by Shi and colleagues (Table S8) [35]. To assess the target association between gastritis and effect of JHT, a "gastritis-targets-symptoms" network for JHT was constructed as shown in Fig. 6A. As a result, 14 targets were found to overlap between the 90 targets for gastritis and 107 targets for the four symptoms; these overlapping targets include CHRM1, CHRM4, TYMS, DRD3, DRD2, TUBB1, HTR1A, HTR2A, PTGS1, PTGS2, AKR1B1, MPO, XDH, and SLC18A2. Except for TYMS, the other 13 targets were recognized to be involved in "pain," indicating that for the treatment of gastritis, "pain" is the most important symptom for drugs approved by the FDA. Notably, DRD2 and AKR1B1 are two of the top three targets in the target screening for "pain." Therefore, when JHT is administered to treat CSG, MMP2, DRD2, and AKR1B1 tend to be its key targets to alleviate symptoms associated with CSG including "chi," "blood," "pain," and "inflammation."

The signaling pathways containing the three targets (MMP2, DRD2, and AKR1B1) were extracted from the results of GSEA analysis (Table S6). As shown in Fig. 6B, four signaling pathways were affected by MMP2. Previously, the transendothelial migration of T cells into the gastric mucosa was found to be strongly associated with *Helicobacter pylori* infection and thus caused active chronic gastritis [36]. Inhibiting MMP2 tended to be an effective approach to attenuating the signaling pathway of "leukocyte transendothelial migration" and enable positive regulation of gastritis. Two signaling pathways were found to be affected by DRD2. The "neuroactive ligand-receptor interaction" between dopamine and DRD2 is known to play a role in the modulation of nociceptive transmission [37]. Moreover, the antagonists of DRD2

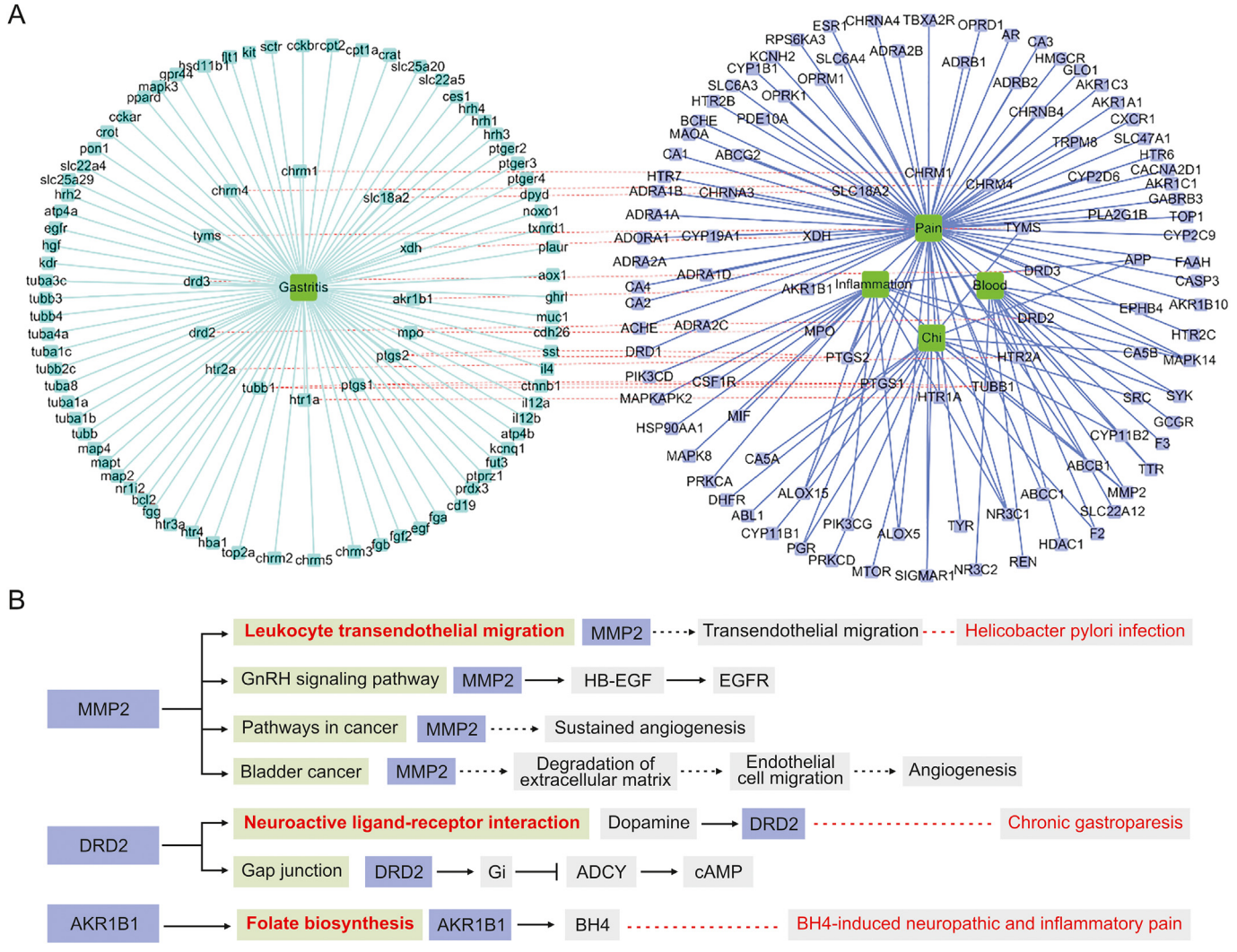

Fig. 6. The key targets and signaling pathways associated with gastritis. (A) "Gastritis-targets-symptoms" network for targets involved in gastritis and the four symptoms ("chi," "blood," "pain," and "inflammation"). Gastritis and the four symptoms, targets of gastritis, and the targets of the four symptoms are represented by green, blue, and cyan nodes, respectively. Target labels for gastritis and the four symptoms are presented in lowercase and uppercase letters, respectively; a red dash has been used to connect the two features. (B) The key signaling pathways regulated by MMP2, DRD2, and AKR1B1. The key pathways and their association with gastritis are displayed in red bold and are connected by a red dash.

(such as “domperidone”) alleviate severe symptoms (nausea and vomiting) associated with chronic gastroparesis and are effective at inducing gastric emptying [38,39]. AKR1B1 was only found to affect the “folate biosynthesis” signaling pathway, which has a direct effect on the levels of BH4 (tetrahydrobiopterin). Based on animal experiments performed with mice, axotomized sensory neurons and macrophages infiltrating damaged nerves and inflamed tissue could produce excessive BH4, thereby increasing sensitivity to pain [40]. The inhibition of AKR1B1 could thus block BH4 production and reduce nerve injury-induced hypersensitivity without affecting nociceptive pain. Collectively, these findings highlight the involvement of MMP2, DRD2, and AKR1B1 in the specific signaling pathways that might interact with or be regulated by the compounds identified in JHT to successfully treat gastritis.

3.4. The inhibitory activities of representative compounds in JHT against MMP2, DRD2, and AKR1B1 and an analysis of their binding modes

The compounds interacting with MMP2, DRD2, and AKR1B1 that had possibilities of 1.0 were extracted from the interaction prediction in the SwissTargetPrediction server (Table S4). Thereafter, their inhibitory activities (Table 2) were derived from the CHEMBL database (https://www.ebi.ac.uk/chembl/) [41–45]. A refined pharmacological network (Fig. 7A) composed of herbs, compounds, targets, and symptoms was constructed to reveal the therapeutic effect of JHT against CSG. The binding modes of the native ligands and representative compounds against the key targets (MMP2, DRD2, and AKR1B1) were analyzed and presented in Figs. 7B–D and Figs. S15–S18.

Chlorogenic acid (**10**), isochlorogenic acid A (**41**), quercetin-3-*O*-α-L-rhamnoside (**42**), isochlorogenic acid B (**47**), quercetin (**63**), and kaempferol (**70**) had inhibitory activities against AKR1B1, with IC_{50} values of 300, 88, 150, 78, 2200, and 10,000 nM, respectively (Table 2). Moreover, these components were found to mainly interact with the catalytic site of AKR1B1, which is located next to the cofactor, $NADP^+$ (Fig. S15). Based on binding mode analysis (Fig. 7B), isochlorogenic acid B (**47**) interacted with the pocket residues of AKR1B1, including Tyr48, His110, Trp111, Thr113, Phe115, Phe122, Leu124, Trp219, Cys298, Ala299, Leu300, and Tyr309. Among these residues, Tyr48, His110, and Trp111 formed hydrogen bonds with isochlorogenic acid B (**47**). (−)-corydalmine (**33**) and (−)-isocorypalmine (**36**) belong to the tetrahydroprotoberberine alkaloids and have been predicted to interact with DRD2 (Table 2). A series of structural analogs of **33** and **36** were previously reported to exhibit antagonistic activities against DRD2 [46]. Herein, the antagonists of DRD2 were found to mainly interact with the substrate-binding site located inside of seven transmembrane helixes (Fig. S16). As shown in Fig. 7C, (−)-isocorypalmine (**36**) interacted with residues, including Val91, Alu94, Asp114, Ile184, Phe189, Ser193, Trp407, Phe410, Phe411, Thr433, and Tyr437. Of these residues, Ser193 and Asp114 formed hydrogen bonds and electrostatic interactions with isocorypalmine (**36**). Caffeic acid (**13**) and quercetin (**63**) were found to exhibit inhibitory activities against MMP2, with IC_{50} values of 24.26 nM and 6680 nM, respectively (Table 2). These MMP2 inhibitors mainly interacted with the catalytic site adjacent to the cofactor, Zn^{2+} (Fig. S17). As shown in Fig. 7D, caffeic acid (**13**) interacted with MMP2 via Leu83, Ala84, Val117, His120, Glu121, His130, and Tyr142. Further, this compound (**13**) was found to form hydrogen bonds with Glu121 and electrostatic interactions with Zn^{2+}.

According to the analysis above, organic acids and flavonoids were found to exhibit inhibitory activities against AKR1B1 and MMP2, while alkaloids exhibited antagonistic activities against DRD2; these compounds belong to the three main structural types in JHT. Through pharmacological studies on chlorogenic acid (**10**) [47,48], caffeic acid (**13**) [49,50], (−)-corydalmine (**33**), (−)-isocorypalmine (**36**) [51,52], quercetin (**63**) [53], and kaempferol (**70**) [54,55], a direct relationship was found between the pharmacodynamic activities of these components in JHT and the therapeutic effects exhibited in gastritis cases. These representative compounds exhibited inhibitory activities against MMP2, DRD2, and AKR1B1, ultimately revealing the comprehensive regulatory effect of JHT against gastritis.

3.5. Biological insights from bioinformatics analysis and implications for novel drug usage to treat CSG

Because TCM prescriptions include a combination of multiple Chinese herbs, it is difficult to associate their therapeutic effect with their molecular basis. Based on the data of approved drugs and their interacting targets in the Drugbank database (https://go.drugbank.com/), a connection can be established between the corresponding symptoms of Chinese herbs and the therapeutic effects of Western medicine. In the TCM theory, most Chinese medicine herbs exhibit effects that are associated with “chi,” “blood,” “pain,” and “inflammation.” As a result, a target collection based on these symptoms would be useful in assessing other TCM prescriptions containing Chinese herbs that exhibit the same effects.

To identify the molecular mechanism employed by JHT in the treatment of CSG, the key targets of JHT must be screened. Targets such as AKR1B1, DRD2, and MMP2 are known to have a close

Table 2
Chemical components of JHT that could interact with MMP2, DRD2, and AKR1B1 and their validated activities.

Compounds	Structural types	Targets[a]	Possibilities[b]	Inhibitory activities[c] (nM)	Refs.
Chlorogenic acid (**10**)	Organic acids	AKR1B1	1.00	300	[41]
Caffeic acid (**13**)	Organic acids	MMP2	1.00	24.26	[42]
(−)-Corydalmine (**33**)	Alkaloids	DRD2	1.00	N/A[d]	N/A
(−)-Isocorypalmine (**36**)	Alkaloids	DRD2	1.00	N/A	N/A
Isochlorogenic acid C (**38**)	Organic acids	AKR1B1	1.00	N/A	N/A
Isochlorogenic acid A (**41**)	Organic acids	AKR1B1	1.00	88	[41]
Quercetin-3-*O*-α-L-rhamnoside (**42**)	Flavonoids	AKR1B1	1.00	150	[43]
Isochlorogenic acid B (**47**)	Organic acids	AKR1B1	1.00	78	[41]
Quercetin (**63**)	Flavonoids	MMP2/AKR1B1	1.00	6680/2200	[44,45]
Kaempferol (**70**)	Flavonoids	AKR1B1	1.00	10,000	[45]

[a] A compound may interact with one or more targets.
[b] The interaction probabilities between compounds and targets. A value of 1.00 indicates an explicit interaction according to the prediction in SwissTargetPrediction.
[c] The inhibitory activities (IC_{50}) between compounds and targets were retrieved from the CHEMBL database (https://www.ebi.ac.uk/chembl/) and relevant literature.
[d] N/A indicates the unavailability of data for the inhibitory activities (IC_{50}).

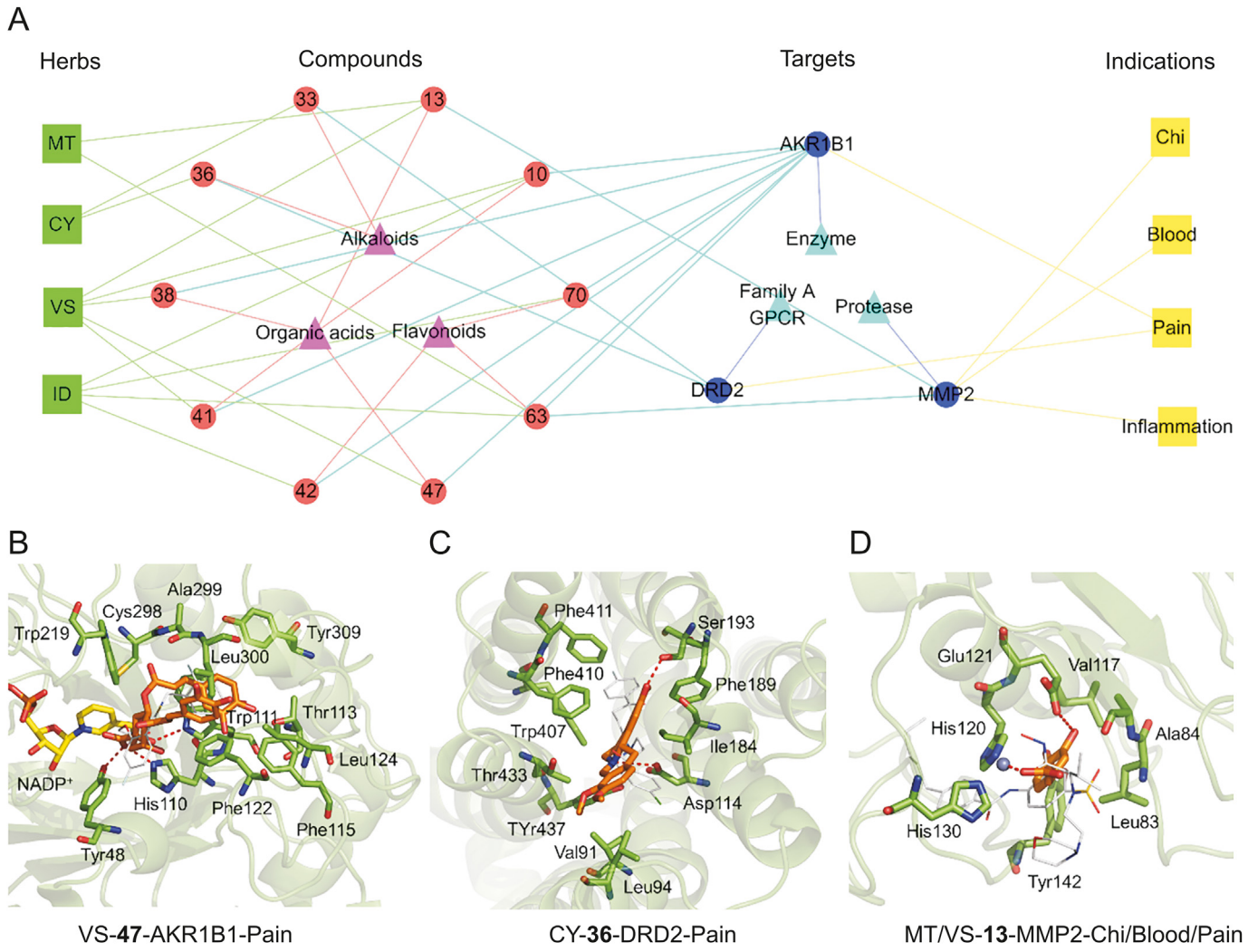

Fig. 7. The refined pharmacological network regulated by MMP2, DRD2, and AKR1B1 and the binding modes between the representative compounds and the three targets. (A) The refined pharmacological network for JHT. The nodes representing herbs, compounds, targets, symptoms, compound types, and target types are displayed as green square, red circle, blue circle, yellow square, purple triangle, and cyan triangle, respectively. The edges between different nodes are presented in different colors. (B) Binding modes for isochlorogenic acid B (**47**) and AKR1B1. The original ligand (IDD594), cofactor ($NADP^+$), isochlorogenic acid B (**47**), and residues on AKR1B1 are displayed as white lines, yellow sticks, orange sticks, and green sticks, respectively. (C) Binding modes for (−)-isocorypalmine (**36**) and DRD2. The original ligand (risperidone), (−)-isocorypalmine (**36**), and residues on DRD2 are displayed as white lines, orange sticks, and green sticks, respectively. (D) Binding modes for caffeic acid (**13**) and MMP2. The original ligand (SC-74020), cofactor (Zn^{2+}), caffeic acid (**13**), and residues on AKR1B1 are displayed as white lines, yellow sticks, blue balls, and green sticks, respectively. All hydrogen bonding and electrostatic interactions are presented as a red dash.

relationship with gastritis. In fact, when the chemical components in JHT interact with these three targets, CSG is regulated via "leukocyte transendothelial migration," "neuroactive ligand-receptor interaction," and "folate biosynthesis," which affect the biological factors of CSG, including "*Helicobacter pylori* infection," "chronic gastroparesis," and "BH4-induced neuropathic and inflammatory pain." When these factors are inhibited by JHT, a synergistic effect against CSG could thus be exerted. A series of compounds in JHT exhibit inhibitory activities against the three targets (i.e., AKR1B1, DRD2, and MMP2) and display a direct pharmacodynamic association with gastritis. As a result, these compounds could serve as quality markers for qualitative evaluation of JHT.

4. Conclusions

In the present study, we sought to systematically characterize the chemical profiles of JHT via UPLC-Q-TOF/MS and predict its molecular mechanisms via a symptom-guided network pharmacology analysis. Herein, 96 compounds were identified in JHT, including 28 alkaloids, 20 organic acids, 16 sesquiterpenoids, 13 triterpenoids, 8 flavonoids, 4 phenylpropanoids, and 7 other compounds. In addition, 31 constituents were confirmed using reference standards. Based on the symptom-guided pharmacological network analysis, MMP2, DRD2, and AKR1B1 were identified as key targets for JHT to exhibit its effects against CSG. Alkaloids, flavonoids, and organic acids such as chlorogenic acid (**10**), caffeic acid (**13**), (−)-corydalmine (**33**), (−)-isocorypalmine (**36**), isochlorogenic acid C (**38**), isochlorogenic acid A (**41**), quercetin-3-*O*-α-L-rhamnoside (**42**), isochlorogenic acid B (**47**), quercetin (**63**), and kaempferol (**70**) tend to show comprehensive activities against gastritis by interacting with the above targets in four symptoms associated with CSG. Altogether, we applied an effective approach to reveal the relationship between the chemical components and effects of JHT against CSG. Such findings could serve as a basis for further research and application of JHT as a clinical treatment.

CRediT author statement

Danfeng Shi: Writing - Original draft preparation, Formal analysis, Visualization; **Lingxian Liu:** Writing - Original draft preparation, Investigation, Data curation, Validation; **Haibo Li:** Writing - Reviewing and Editing, Visualization; **Dabo Pan:** Investigation; **Xiaojun Yao:** Software; **Wei Xiao:** Resources, Conceptualization, Funding acquisition; **Xinsheng Yao:** Resources, Project administration, Conceptualization, Supervision; **Yang Yu:** Writing - Reviewing and Editing, Conceptualization, Methodology, Supervision.

Declaration of competing interest

The authors declare that there are no conflicts of interest.

Acknowledgments

This research was funded by the National Natural Science Foundation of China (Grant Nos.: 81903426 and 81803347). We are grateful for the high-performance computing platform at Jinan University, China, which was used to carry out this study.

Appendix A. Supplementary data

Supplementary data to this article can be found online at https://doi.org/10.1016/j.jpha.2021.01.005.

References

[1] J.-Y. Fang, Y.Q. Du, W.Z. Liu, et al., Chinese consensus on chronic gastritis (2017, Shanghai), J. Dig. Dis. 19 (2018) 182–203.
[2] P. Sipponen, H.-I. Maaroos, Chronic gastritis, Scand. J. Gastroenterol. 50 (2015) 657–667.
[3] M. Stolte, A. Meining, The updated Sydney system: classification and grading of gastritis as the basis of diagnosis and treatment, Can. J. Gastroenterol. 15 (2001) 591–598.
[4] E.J. Kuipers, A.M. Uyterlinde, A.S. Peña, et al., Long-term sequelae of Helicobacter pylori gastritis, Lancet 345 (1995) 1525–1528.
[5] M. Varbanova, K. Frauenschläger, P. Malfertheiner, Chronic gastritis - an update, Best Pract. Res. Clin. Gastroenterol. 28 (2014) 1031–1042.
[6] L.H. Osaki, K.A. Bockerstett, C.F. Wong, et al., Interferon-γ directly induces gastric epithelial cell death and is required for progression to metaplasia, J. Pathol. 247 (2019) 513–523.
[7] X.-L. Wang, Re-discussing the advantage of TCM in treating infectious diseases, J. Tianjin Univ. Tradit. Chin. Med. 30 (2011) 193–195 (in Chinese).
[8] F. Chen, Clinical observation on treatment of chronic superficial gastritis with Jinhong tablets and ranitidine, Chin. J. Clin. Ration. Drug Use 3 (2010), 69 (in Chinese).
[9] J. Zhang, J. Song, L. Zhang, et al., Observation on therapeutic effect of 325 cases of chronic superficial gastritis with disharmony of liver and stomach treated by Jinhong tablets, Chin. J.Tradit. Med. Sci. Technol. 5 (1998) 251 (in Chinese).
[10] H. Matsuda, K. Tokuoka, J. Wu, et al., Inhibitory effects of methanolic extract from corydalis tuber against types I-IV allergic models, Biol. Pharm. Bull. 18 (1995) 963–967.
[11] M. Kubo, H. Matsuda, K. Tokuoka, et al., Anti-inflammatory activities of methanolic extract and alkaloidal components from Corydalis tuber, Biol. Pharm. Bull. 17 (1994) 262–265.
[12] H. Zheng, Y. Chen, J. Zhang, et al., Evaluation of protective effects of costunolide and dehydrocostuslactone on ethanol-induced gastric ulcer in mice based on multi-pathway regulation, Chem. Biol. Interact. 250 (2016) 68–77.
[13] F. Xie, M. Zhang, C.-F. Zhang, et al., Anti-inflammatory and analgesic activities of ethanolic extract and two limonoids from Melia toosendan fruit, J. Ethnopharmacol. 117 (2008) 463–466.
[14] T. Shi, Z. Yao, Z. Qin, et al., Identification of absorbed constituents and metabolites in rat plasma after oral administration of Shen-Song-Yang-Xin using ultra-performance liquid chromatography combined with quadrupole time-of-flight mass spectrometry, Biomed. Chromatogr. 29 (2015) 1440–1452.
[15] J.-L. Geng, Y. Dai, Z.-H. Yao, et al., Metabolites profile of Xian-Ling-Gu-Bao capsule, a traditional Chinese medicine prescription, in rats by ultra performance liquid chromatography coupled with quadrupole time-of-flight tandem mass spectrometry analysis, J. Pharm. Biomed. Anal. 96 (2014) 90–103.
[16] Z.-F. Qin, Y. Dai, Z.-H. Yao, et al., Study on chemical profiles and metabolites of Allii Macrostemonis Bulbus as well as its representative steroidal saponins in rats by ultra-performance liquid chromatography coupled with quadrupole time-of-flight tandem mass spectrometry, Food Chem. 192 (2016) 499–515.
[17] A.L. Hopkins, Network pharmacology, Nat. Biotechnol. 25 (2007) 1110–1111.
[18] A.L. Hopkins, Network pharmacology: the next paradigm in drug discovery, Nat. Chem. Biol. 4 (2008) 682–690.
[19] W. Zhu, Z. Fan, G. Liu, et al., Symptom clustering in chronic gastritis based on spectral clustering, J. Tradit. Chin. Med. 34 (2014) 504–510.
[20] Q. Wang, S. Yao, Molecular basis for cold-intolerant yang-deficient constitution of traditional Chinese medicine, Am. J. Chin. Med. 36 (2008) 827–834.
[21] S. Li, Z.Q. Zhang, L.J. Wu, et al., Understanding ZHENG in traditional Chinese medicine in the context of neuro-endocrine-immune network, IET Syst. Biol. 1 (2007) 51–60.
[22] S. Li, Exploring traditional Chinese medicine by a novel therapeutic concept of network target, Chin. J. Integr. Med. 22 (2016) 647–652.
[23] K. Wang, L. Chai, X. Feng, et al., Metabolites identification of berberine in rats using ultra-high performance liquid chromatography/quadrupole time-of-flight mass spectrometry, J. Pharm. Biomed. Anal. 139 (2017) 73–86.
[24] C. Dai, C. Wang, C. Zhang, et al., A reference substance free diagnostic fragment ion-based approach for rapid identification of non-target components in Pudilan Xiaoyan oral liquid by high resolution mass spectrometry, J. Pharm. Biomed. Anal. 124 (2016) 79–92.
[25] L. He, Z. Qin, M. Li, et al., Metabolic profiles of ginger, a functional food, and its representative pungent compounds in rats by ultraperformance liquid chromatography coupled with quadrupole time-of-flight tandem mass spectrometry, J. Agric. Food Chem. 66 (2018) 9010–9033.
[26] A. Daina, O. Michielin, V. Zoete, SwissTargetPrediction: updated data and new features for efficient prediction of protein targets of small molecules, Nucleic Acids Res. 47 (2019) W357–W364.
[27] D.S. Wishart, Y.D. Feunang, A.C. Guo, et al., DrugBank 5.0: a major update to the DrugBank database for 2018, Nucleic Acids Res. 46 (2018) D1074–D1082.
[28] Z.-X. Qing, P. Cheng, X.-B. Liu, et al., Systematic identification of alkaloids in Macleaya microcarpa fruits by liquid chromatography tandem mass spectrometry combined with the isoquinoline alkaloids biosynthetic pathway, J. Pharm. Biomed. Anal. 103 (2015) 26–34.
[29] D.C. Wallace, Mitochondria as chi, Genetics 179 (2008) 727–735.
[30] M. Picard, D.C. Wallace, Y. Burelle, The rise of mitochondria in medicine, Mitochondrion 30 (2016) 105–116.
[31] D. Singh, S.K. Srivastava, T.K. Chaudhuri, et al., Multifaceted role of matrix metalloproteinases (MMPs), Front. Mol. Biosci. 2 (2015), 19.
[32] P.J. Bergin, E. Anders, S. Wen, et al., Increased production of matrix metalloproteinases in Helicobacter pylori-associated human gastritis, Helicobacter 9 (2004) 201–210.
[33] H.I. Rautelin, A.M. Oksanen, L.I. Veijola, et al., Enhanced systemic matrix metalloproteinase response in Helicobacter pylori gastritis, Ann. Med. 41 (2009) 208–215.
[34] C.L. Sampieri, S. de la Peña, M. Ochoa-Lara, et al., Expression of matrix metalloproteinases 2 and 9 in human gastric cancer and superficial gastritis, World J. Gastroenterol. 16 (2010) 1500–1505.
[35] G. Yu, W. Wang, X. Wang, et al., Network pharmacology-based strategy to investigate pharmacological mechanisms of Zuojinwan for treatment of gastritis, BMC Complement. Altern. Med. 18 (2018), 292.
[36] K. Enarsson, M. Brisslert, S. Backert, et al., Helicobacter pylori induces transendothelial migration of activated memory T cells, Infect. Immun. 73 (2005) 761–769.
[37] S. Potvin, S. Grignon, S. Marchand, Human evidence of a supra-spinal modulating role of dopamine on pain perception, Synapse 63 (2009) 390–402.
[38] A. Sturm, G. Holtmann, H. Goebell, et al., Prokinetics in patients with gastroparesis: a systematic analysis, Digestion 60 (1999) 422–427.
[39] H. Abrahamsson, Treatment options for patients with severe gastroparesis, Gut 56 (2007) 877–883.
[40] A. Latremoliere, A. Latini, N. Andrews, et al., Reduction of neuropathic and inflammatory pain through inhibition of the tetrahydrobiopterin pathway, Neuron 86 (2015) 1393–1406.
[41] M. Soda, D. Hu, S. Endo, et al., Design, synthesis and evaluation of caffeic acid phenethyl ester-based inhibitors targeting a selectivity pocket in the active site of human aldo–keto reductase 1B10, Eur. J. Med. Chem. 48 (2012) 321–329.
[42] Z.-H. Shi, N.-G. Li, Q.-P. Shi, et al., Synthesis and structure–activity relationship analysis of caffeic acid amides as selective matrix metalloproteinase inhibitors, Bioorg. Med. Chem. Lett. 23 (2013) 1206–1211.
[43] U. Dhagat, S. Endo, A. Hara, et al., Inhibition of 3 (17) α-hydroxysteroid dehydrogenase (AKR1C21) by aldose reductase inhibitors, Bioorg. Med. Chem. 16 (2008) 3245–3254.
[44] L. Wang, X. Li, S. Zhang, et al., Natural products as a gold mine for selective matrix metalloproteinases inhibitors, Bioorg. Med. Chem. 20 (2012) 4164–4171.
[45] S. Naeem, P. Hylands, D. Barlow, Construction of an Indonesian herbal constituents database and its use in Random Forest modelling in a search for inhibitors of aldose reductase, Bioorg. Med. Chem. 20 (2012) 1251–1258.
[46] G. Jin, Q. Zhou, L. Chen, et al., New pharmacological effects of tetrahydroprotoberberines on doapmine receptor, Bull. Nat. Sci. Found. China 5 (2000) 300–304.
[47] A. Marengo, M. Fumagalli, C. Sanna, et al., The hydro-alcoholic extracts of Sardinian wild thistles (Onopordum spp.) inhibit TNFα-induced IL-8 secretion and NF-κB pathway in human gastric epithelial AGS cells, J. Ethnopharmacol. 210 (2018) 469–476.
[48] B.W. Bang, D. Park, K.S. Kwon, et al., BST-104, a water extract of *Lonicera*

japonica, has a gastroprotective effect via antioxidant and anti-inflammatory activities, J. Med. Food 22 (2019) 140–151.
[49] F.M. da Cunha, D. Duma, J. Assreuy, et al., Caffeic acid derivatives: in vitro and in vivo anti-inflammatory properties, Free Radic. Res. 38 (2004) 1241–1253.
[50] W.S. Yang, D. Jeong, Y.-S. Yi, et al., IRAK1/4-targeted anti-inflammatory action of caffeic acid, Mediators Inflamm. (2013), 518183.
[51] L. Zhou, Y. Hu, C. Li, et al., Levo-corydalmine alleviates vincristine-induced neuropathic pain in mice by inhibiting an NF-kappa B-dependent CXCL1/CXCR2 signaling pathway, Neuropharmacology 135 (2018) 34–47.
[52] Z.-Z. Ma, W. Xu, N.H. Jensen, et al., Isoquinoline alkaloids isolated from Corydalis yanhusuo and their binding affinities at the dopamine D1 receptor, Molecules 13 (2008) 2303–2312.
[53] S. Zhang, J. Huang, X. Xie, et al., Quercetin from *Polygonum capitatum* protects against gastric inflammation and apoptosis associated with *Helicobacter pylori* infection by affecting the levels of p38MAPK, BCL-2 and BAX, Molecules 22 (2017), 744.
[54] M.J. Yeon, M.H. Lee, D.H. Kim, et al., Anti-inflammatory effects of Kaempferol on Helicobacter pylori-induced inflammation, Biosci. Biotechnol. Biochem. 83 (2019) 166–173.
[55] S.H. Kim, J.G. Park, G.-H. Sung, et al., Kaempferol, a dietary flavonoid, ameliorates acute inflammatory and nociceptive symptoms in gastritis, pancreatitis, and abdominal pain, Mol. Nutr. Food Res. 59 (2015) 1400–1405.